Dynamical downscaling of wind resource in complex terrain prone to downslope windstorms: the case of Croatia

Authors: Kristian Horvath[1], Alica Bajić[1], Stjepan Ivatek-Šahdan[1]
[1]Meteorological and Hydrological Service, Grič 3, 10000 Zagreb, Croatia

Corresponding author: dr.sc. Kristian Horvath, Grič 3, 10000 Zagreb, Croatia
Tel: +385-1-4565752
Fax: +385-1-4565630
Email: kristian.horvath@cirus.dhz.hr

Abstract

The results of climatologically representative spatial distribution of wind speed, a primary component of wind energy resource assessment in complex terrain of Croatia, are given in the paper. For that purpose, dynamical downscaling of 10 years of ERA40 reanalysis (1992-2001) was performed to 8 km horizontal grid resolution with the use of spectral, prognostic full-physics model ALADIN (ALHR). Subsequently, model data with a 60-min frequency was refined to a 2 km horizontal grid resolution with a simplified model version, so-called dynamical adaptation (DADA).

The statistical verification of ERA40, ALHR and DADA modelled wind speed, performed on measurement stations representing different wind climate regimes of Croatia, suggests that downscaling was successful and that overall model accuracy systematically increases with the increase of horizontal resolution. The areas of the highest wind resource correspond well to locations of frequent and strong bora flow as well as the prominent mountain peaks. The best results, with bias equalling 1% of the mean wind speed in the eastern Croatia and close to 10 % in coastal complex terrain, are achieved with DADA, illustrating the added value of computationally considerably less expensive dynamical adaptation to wind resource estimates. Root-mean square errors of DADA are significantly smaller in flat than in complex terrain, while relative values are close to 12% of the mean wind speed regardless of the station location.

Spectral analysis was performed in both spatial and temporal domains, illustrating model success on a variety of scales. The shape of kinetic energy spectrum generally relaxes from k^{-3} at the upper-troposphere to $k^{-5/3}$ near the surface and confirms unique as regard to season. Apart from build-up of energy on smaller scales of motions, it is shown that mesocale simulations contain a considerable amount of energy related to near-surface mostly divergent meso-β (20-200 km) motions. Spectral decomposition of measured and modelled data in temporal space indicates a reasonable performance of all model datasets in simulating the primary maximum of spectral power related to synoptic motions, with somewhat increased accuracy of the mesoscale model data. Secondary diurnal and terciary semidiurnal maxima, associated with the land/sea breeze and slope circulations, are significantly better simulated with the mesoscale model on coastal stations, while being somewhat more erroneous on the continental station. Finally, it is shown mesoscale

model data underestimates the spectral power of motions with less-then-semidiurnal periods.

1. Introduction

The wind climatology is the crucial factor for establishing the meteorological basis for the assessment of wind energy resources. Typically, global reanalysis data, available on ~100 km horizontal grid resolution or more, is not satisfactorily accurate for assessment of the wind climate in planetary boundary layer, especially over complex terrain. Therefore, this data needs to be downscaled over the target area during a substantially long period, in order to attain spatial and temporal representativeness. One of the common methods for estimation of wind climate in complex terrain, especially in areas of scarce or inexistent high-quality measurements, is dynamical downscaling with the use of mesoscale numerical weather prediction models. The spatial and temporal refinement of wind climate depends on the target mesoscale model resolution, which should be chosen using knowledge of spatial and temporal scales of the atmospheric phenomena taking place in the target area.

A dynamical downscaling is expected to introduce additional (smaller) spatial and temporal scales, resulting in more adequate reproduction of mesoscale wind systems that are most often either a result of terrain and surface inhomogenities (land-sea breeze, katabatic winds, valley winds etc.) or of their interaction with the large-scale flow (downslope windstorms, gravity waves, gap flows, wakes etc.). It is the coastal mountainous region of the eastern Adriatic coast, the area of the highest wind resource in Croatia, which is frequently subject to strong wind systems, embedded in a range of intense and interrelated sub-synoptic phenomena in the region (Horvath et al., 2008). In particular, gusty, severe downslope windstorm bora (e.g. Smith, 1985; Klemp and Durran, 1987; Smith, 1987) with hurricane scale gusts that can reach 70 ms^{-1} is especially important for wind energy applications. Indeed, the relevance of the phenomena[1] and considerable research related to Croatian bora (see review by Grisogono and Belušić, 2009) suggests the eastern Adriatic coast might be an excellent target area for evaluation of the mesoscale model performance in complex terrain prone to downslope windstorms.

[1] The areas characterized with bora-type flows include but are not limited to: Southern California, Rocky Mountains, Western slopes of the Andes, Austria, Iceland, New Zealand, Sumatra, Japan, Indonesia, Kurdistan, Russia, etc.

Besides bora, which accounts to the largest portion of wind energy potential in the target region, another wind system of importance which blows along the eastern Adriatic coast is southeasterly "jugo"[2] wind. The nature of bora and "jugo", which are strongly determined by the orographic pressure perturbation, suggests that the ability of mesoscale models to simulate non-linear flows and flows over the mountains in different regimes of background flow[3] is an important and desired feature relevant for the success of modelling the representative wind climate or estimating regional wind resource.

Since the power output of a wind turbine is proportional to the third power of the wind speed, the precision requirements for wind speed climatology for energy assessment are higher than for most other purposes. Despite the widespread use of mesoscale models, verification of their performance is a challenging issue, which often does not follow a unified approach. The statistical verification which uses basic verification parameters (e.g. systematic error, root-mean square error, etc.) seems to be only partially sufficient for the purpose, since small errors in time or location of the otherwise well simulated particular phenomena can overwhelmingly deprive the verification scores (Mass et al., 2002).

Therefore it is often favourable to utilize a complimentary analysis and verification method, such as the spectral analysis, that can provide scale-dependent measure of model performance. For example, the evaluation of power spectra from measured and modelled timeseries facilitates the evaluation of model performance on different temporal scales, such as synoptic, mesoscale, diurnal, semidiurnal and sub-semidiurnal. On the other hand, the success of models to simulate the proper shape of kinetic energy spectrum in spatial domain can serve as a prime tool for qualitative model evaluations.

The primary goal of this paper is to present results of the performed dynamical downscaling over a 10-year period with the use of the mesoscale model ALADIN as well as to assess the ability of the mesoscale model to reproduce the relevant wind speed

[2] "Jugo" is a local name for a southeasterly wind that takes place over the wider region of the Adriatic Sea. It belongs to the family of southwesterly Mediterranean sirocco winds, which are channeled to the southeasterly direction by the Dinaric Alps (Jurčec et al., 1996).

[3] Background flow – the flow impinging on the mountain – to the first approximation (together with mountain height and shape) determines the lee-side responce. Its properties of primary importance are cross-mountain wind speed component and (moist) static stability.

climate in complex terrain of Croatia as a basis for wind energy assessment. This is achieved by means of statistical and spectral verification at selected stations. Furthermore, spatial spectra of the kinetic energy, vorticity and divergence are used to study the ability of the ALADIN model to reproduce universally observed spectra in the free troposphere, but also to study the mesoscale spectra at near-surface levels, relevant to wind energy applications.

The paper is organized as follows. The methodology is described in Section 2. The results of the dynamical downscaling are presented in Section 3, while statistical and spectral analysis and verification are presented in Section 4. Finally, conclusions are given in Section 5.

2. Methodology

Dynamical downscaling was performed with the mesoscale model ALADIN (Bubnova et al., 1995), which is used for everyday numerical weather prediction typically at 5-10 km resolutions in over a dozen of countries (http://www.cnrm.meteo.fr/aladin/). ALADIN is a primitive equation spectral model with hybrid η coordinate (Simmons and Burridge, 1981), with a two-time-level semi-implicit semi-lagrangian scheme. Model fields in spectral space are obtained by double Fourier transform, and the bi-periodicity is satisfied by introducing the extension zone (Machenhauer and Haugen, 1987). Davies (1976) relaxation scheme is used for coupling with the driving model. Physical parameterizations include vertical diffusion (Louis et al., 1982) and shallow convection (Geleyn, 1987). Kessler type of parameterization is used to account for resolved precipitation (Kessler, 1969) and deep convection is modelled with a modified Kuo scheme (Geleyn et al., 1982). Radiation is described following Geleyn and Hollingsworth (1979) and Ritter and Geleyn (1992). Two-layer soil scheme (Giard and Bazile, 2000) is used to simulate vertical transport of soil moisture and heat.

Model is run in a hydrostatic mode with 37 vertical levels (the lowest model level at 17 m) and 8 km horizontal grid resolution. The model domain is shown on Fig. 1. Initial and boundary conditions were provided by the global reanalysis of the European Centre for Medium-Range Forecast (ECMWF) ERA-40 (Kållberg et al., 2004), available at 125 km grid resolution with a 6 hourly frequency. Following Beck et al. (2004) and Žagar et al. (2006) a direct nesting strategy was implemented. Namely, they have snowed that the dynamical downscaling of ERA-40 data with the ALADIN model to ~10 km grid resolution was equally accurate whether or not an intermediate domain is used. Though there is no doubt that in some individual cases and events this nesting ratio would show rather excessive, it appears that for wind resource estimate the proposed approach holds sufficient, yet cost-effective. Prior to integration, data was interpolated in space and filtered using digital filter initialization procedure (Lynch and Huang, 1994). The model was initialized daily at 12 UTC and run for the 36 hours, while the output data was archived with 60-min frequency. Due to the large grid ratio, a 12-hourly spin-up time was provided in order to allow sufficient time for build up of mesoscale energy in the model

(Žagar et al., 2006).

Upon integration, 24-hourly period starting with 12-hourly forecast range was refined to 2 km model grid on a sub-domain (Fig. 1) with so-called "dynamical adaptation" (Žagar and Rakovec, 1999). Dynamical adaptation is a cost-effective method of dynamically adjusting near-surface winds from low-resolution model to finer mesh with a simplified mesoscale model version, run operationally in Croatia (Ivatek-Šahdan and Tudor, 2004). Several dozens of time steps is usually required in order to reach the state of dynamical adjustment, which is achieved with the use of time-invariant lateral boundary conditions from the driver model. It typically results in dynamically adjusted near-surface winds considerably faster compared to full model integration at the same grid resolution. Typically, dynamic adaptation will be more effective when pressure gradients are stronger, which suits well the wind resource studies well, especially in terrain prone to strong bora flows. While a more comprehensive description of dynamical adaptation can be found in Žagar and Rakovec (1999), here we describe the model setup: the simplified model version was run for 30 time steps (of 60 seconds), with reduced number of vertical levels above PBL and with all parameterizations withheld, but the parameterization of vertical diffusion.

3. Results

3.1 Spatial distribution of mean wind speed

Mean 10-yearly wind speed at 10 m AGL over the downscaling period (1992-2001) is shown on Fig. 2. The main feature of the spatial distribution is considerably higher wind speed in the wider coastal area and hinterlands than in the continental part of Croatia. The highest mean wind speed over the land is simulated over the eastern slopes of the Velebit mountain, including the proximate areas above the sea, as well as over the higher ridges and mountain tops. While mountain-tops are often regions of enhanced wind resource due to their altitude, the high wind resource area over the western slopes of the Velebit mountain results primarily from the climatologically high frequency of bora (Yoshino, 1976; Bajić, 1989; Poje, 1992; Cavaleri et al., 1997). The channelling of the northeasterly background flow during bora events through the Vratnik pass (e.g. Makjanić, 1976; Göhm et al., 2008) contributes to highest wind resource in the very area. This lee-side maximum extends offshore reaching the outermost islands, acquiring spatial distribution that resembles hydraulic solutions for bora flows (e.g. Smith, 1985) and reaching absolute maximum of mean near-surface wind speed close to 6.5 ms^{-1}. On the other hand, spatial confinement of the lee-side maxima to the very vicinity of the western slopes of southern Velebit, indicates the preference for the other mechanism applicable to strong bora flows, which is related to upstream blocking and gravity wave-breaking (e.g. Klemp and Duran, 1987). The inexistence of such a maximum over the western slopes of southern Dinaric Alps can be associated with the climatologically lower frequency of favourable synoptic setting for the onset of bora, but also with their lower predictability characterized with weaker model performance over the middle and southern Adriatic and related underestimation of strong bora flows (Horvath et al., 2009). Finally, the regions with the weakest 10-yearly mean wind speed are primarily some of the lowland areas of continental Croatia.

These results suggest that bora downslope windstorms are extremely important for wind energy utilization in the coastal part of Croatia. However, due to its gusty character and extreme turbulence which may result in turbulent kinetic energy over 30 Jkg^{-1} (Belušić and Klaić, 2006), estimates of wind resource in the region have to include the properties of bora turbulence. Therefore, higher resolution modelling and more insight into the bora turbulence seem to be the future not only of scientific advancements in the broad area of bora-type flows, but also of relevant wind energy applications in complex terrain.

3.2 Statistical verification

Statistical model verification was performed for ERA40, ALHR and DADA datasets using measured wind speed data during 2001 from 4 meteorological stations (cf. Fig. 1) that represent different climate regimes of Croatia. The station of Slavonski Brod (SLB) is representative of moderate continental climate and in the vicinity of gently sloped terrain. Stations Novalja (NOV), Split Marjan (STM) and Dubrovnik (DUB) were selected to assess model verification in maritime climate (e.g. Zaninović et al., 2008), characterized with the proximity of Dinaric Alps. Model data was bilinearly interpolated to the station locations without any other post-processing. Instrument errors, calibration errors and representativeness errors were not taken into account during the model verification. This should be also kept in mind when evaluating model performance, since for example the estimate of a representativeness error, which is the highest among the above, equals close to 1 ms^{-1} for near-surface wind speed in well mixed boundary layer in complex terrain (e.g. Rife et al., 2004).

The statistical scores, such as multiplicative systematic error (MBIAS, unity implies no systematic error) and root-mean square error (RMSE) (e.g. Wilks, 1995), for the selected stations are calculated and averaged over monthly periods showing their seasonal variability (Figs. 3, 4), while mean annual values are shown in Table 1. The ALHR and DADA model output data was used with 6-hourly frequency for comparison with ERA40 dataset. The 1-hourly statistical scores for ALHR and DADA models are for reference given in Table 1 and do not show significant differences.

For the continental station SLB, in weakly sloped terrain, annually averaged MBIAS shows a strong overestimation of ERA40 wind speeds, with a yearly mean value of 1.51. The greatest systematic error in present the October (MBIAS=2.59), which is the month with the weakest mean wind (0.82 ms^{-1}). The annual mean of systematic errors for ALHR (0.99) and DADA (1.01) data is significantly improved and nearly negligible, although there does exist an intermonthly variability.

Among the costal stations, ERA40 performs the worst at station NOV with a MBIAS equalling 0.69. Similar to the station SLB, the peak of increased MBIAS is present in October, which is again the month with the weakest mean wind speed (2.7 ms^{-1}). This issue is not a characteristic of ALHR and DADA data, suggesting the overestimation might be due to weaker ability of the ECMWF global model to simulate near-calm wind conditions, perhaps due over diffusive model setup (see Sec. 3.3). The mean annual MBIAS at station NOV significantly improves for ALHR and DADA stations equalling 0.79 and 0.92 respectively. Similarily, MBIAS for station STM improves with higher grid resolution and equals 0.78, 0.85 and 0.89 for ERA40, ALHR and DADA data respectively, with no significant intermonthly variability. However, for station DUB, ERA40 data show no systematic errors and outperforms ALHR and DADA models that underestimate the mean wind speed for 9%. This is likely to be at least partially related to applied bilinear interpolation and the fact that for this land station 3 out of 4 ERA40 data grid points are located over the sea, thus being insufficiently representative of the actual station surroundings. At DUB station, the intermonthly variability of MBIAS is the weakest among all the analysed stations.

The recorded average underestimation of mean wind speed at coastal sites is very likely due the underestimation of stronger wind speed events, where the frequency of weaker winds ($V < 6$ ms^{-1}) is overestimated on the account of the stronger winds ($V > 6$ ms^{-1}). There are several reasons that might contribute to underestimation of stronger winds, such as appropriateness of physical parameterizations, especially the PBL scheme, quality of lower boundary conditions and propagation of synoptic information through the coupling zone. Due to importance of stronger winds for wind climate estimates in the region, the analysis of underlying reasons, which is beyond the scope of the current paper, will play an important role in increasing the accuracy of dynamical downscaling.

Root-mean square error (RMSE) is smaller in nearly flat terrain of continental Croatia than in complex terrain of the eastern Adriatic coast. Thus, RMSE is the smallest at station SLB, where mean annual RMSE of ERA40 data (0.85 ms^{-1}) is strongly improved by dynamical downscaling and equals 0.22 ms^{-1} (ALHR) and 0.19 ms^{-1} (DADA). The least accurate results are achieved for station NOV, located right in the lee of the high and steep southern Velebit, equalling 1.55 ms^{-1} (ERA40), 1.03 ms^{-1} (ALHR) and 0.73 ms^{-1} (DADA). Since this is the area where bora is most directly associated with wave-breaking bora regime, the low predictability of these phenomena is most likely the underlaying reason for weaker RMSE scores at the station. Nevertheless, for stations NOV and STM, the systematic improvement in accuracy is evident, since RMSE of ERA40 data is roughly halved in DADA dataset. In contrast, RMSE scores at DUB station suggest that the higher resolution ALADIN model data at this station are outperformed by the ERA40 data. Nevertheless, a slight increase in model skill is achieved with the use of DADA, compared to ALHR model. The highest intermonthly variability of RMSE is present on station NOV, followed by STM, with largest errors found in the colder part of the year, characterized with higher frequency of stronger winds in the area. Again station DUB appears not to conform to the case of two costal stations farther to the north.

In general, the dynamical downscaling brings the more accurate wind climate estimates than the global model reanalysis, with considerably smaller systematic and root-mean square errors. The higher resolution dynamical downscaling at 2 km grid resolution, carried out with simplified and cost-effective model formulation, clearly outperformed the results at 8 km grid resolution. The above systematic increase in model accuracy is true in both complex terrain of the eastern Adriatic coast and nearly-flat terrain of continental Croatia. While obviously the improvement of lower-boundary conditions is of an importance for this benefit, we note that a non-local influence of an interaction between the atmosphere and complex terrain plays a significant role for model accuracy also in surrounding flat terrain.

3.3 Spectral analysis in spatial domain

It is known that atmospheric kinetic energy spectrum of inherently 2D large-scale motions in free troposphere follows a k^{-3} power law dependency of kinetic energy spectrum on the wavenumber k (e.g. Kraichnan, 1967; Lilly, 1969; Charney, 1971; Boer and Shepherd, 1983; Nastrom and Gage, 1985) with a great universality regardless of the latitude (mid-latitudes), season or the altitude. A less steep $k^{-5/3}$ dependence on the smallest scales is associated with 3D motions on cloud resolving and turbulence scales (Kolmogorov theory). In between these scales however, the mesoscale spectrum is not completely understood, since the motions on mesoscale motions are predominantly 2D, but kinetic energy spectrum is closer to $k^{-5/3}$ (e.g. Gage and Nastrom, 1986; Lindborg, 1999, Skamarock, 2004). Nevertheless, the spectral analysis in spatial domain is appealing for assessment of model performance due to the universality of both theoretical and observational results.

Prior to calculations of the kinetic energy, vorticity and divergence spectra, a spatial subset of ERA-40 data was created to fit exactly the mesoscale model integration domain which was 1920 km wide. Spectra were calculated each 6 hours (the availability of ERA-40 reanalysis) throughout the year 2001. The results of dynamical adaptation were not used this part of evaluation, since the domain used for dynamical adaptation was too prohibitive to attempt comparison with the ERA-40 reanalysis.

Kinetic energy spectrum (normalized) is shown of Fig. 5a for both ERA-40 reanalysis and ALHR data. First, it is evident that the dynamical downscaling created a portion of mesoscale energy on scales below 250 km (thus unresolved by ERA-40 reanalysis). While in the free atmosphere this part of spectrum captures limited amount of energy, the kinetic energy of meso-β (20-200 km) motions on near-surface levels is way greater than at the upper-levels indicating the important energetic of small-scale processes near the surface.

At the upper-troposphere, down to wavelengths of 250 km, ALADIN and ECMWF spectra are almost identical and conform to the k^{-3} law. However, at scales close to 300 km and lower, the spectrum of the ALADIN model does not show a gradual transition towards the less steep behaviour, suggesting that at these scales there is not enough mesoscale energy created near the tropopause. While the underlying reason is not obvious, it might be that model levels are too scarse near the tropopause (vertical resolution at 9 km close to 800 m) to account for mesoscale processes near the troposphere-stratosphere boundary (intrusions and mesoscale portion of the upper-level jet dynamics). This model property was to some extent noticed in other studies of dynamical downscaling with ALADIN model (e.g. Žagar et al., 2006), regardless of the chosen nesting ratio, domain size or chosen initial and boundary conditions.

In the mid-troposphere (700 hPa), ERA40 reanalysis shows less steep dependency than at 300 hPa level. The ALADIN kinetic energy spectra deviates from the k^{-3} relationship as well, and resembles more the $\sim k^{-2}$ in the whole range wavelengths which is unaffected by diffusive end of the spectrum. Similar shape of kinetic energy spectrum is found in the WRF mesoscale model (Skamarock, 2004). The differences between spectra at 700 hPa and 300 hPa suggest that the kinetic energy spectrum in complex terrain might not be completely altitude-independent throughout the free troposphere.

The flattening of the kinetic energy spectrum is even more obvious on near-surface levels, where spectrum is closer to $k^{-5/3}$, illustrating the properties of boundary layer turbulence that is 3-dimensionality of motions. This applies throughout the scales down to and well below 50 km, suggesting the effective model resolution, as inferred by the deviation between the expected and observed kinetic energy spectra at low wavelengths (see Skamarock, 2004), gets higher closer to the ground. While almost identical at upper-levels, kinetic energy spectra of ALADIN and ERA-40 reanalysis diverge on larger and larger scales as approaching the ground. At 1000 hPa, the ERA-40 spectrum begins to loose energy at scales ~600 km, which is close to 5dx of the ERA40 grid resolution. Thus, it appears that while the effective model resolution of the ALADIN model improves as approaching the ground, the opposite holds for ERA40 reanalysis. While the underlying reasons are not obvious, we note that for the purpose of near-surface wind climate or resource estimate, the effective resolution plays an important role in determining the limits of a potential model performance.

Overall, the kinetic energy on scales over hundreds of kilometres is much stronger at the upper-levels than near the surface, regardless of the model. In contrast, on scales slightly over 100 km and less, the kinetic energy of near-surface motions becomes dominant. This clearly implies that high-resolution mesoscale dynamical downscaling, which aims to study near-surface regional wind climate or resource, needs to be highly reliable on scales sufficiently small to account for the considerate amount of energy contained in the near-surface meso-β scales of motion (20-200 km).

The seasonal dependency of kinetic energy spectrum of the ALADIN model is shown on Fig. 5b. The largest amount of kinetic energy is found in winter, followed by spring and autumn, regardless of the level. The kinetic energy during summer is considerably smaller then during the rest of the year, which reflects the weaker upper-level dynamics as well as lower near-surface wind speeds in the region during the warmest season of the year. Regardless of the season, spectra at different levels have similar shape, in accordance with the observational evidence mentioned above.

Spectral energy densities of vorticity and divergence at the upper-troposphere (300 hPa), mid-troposphere (700 hPa) and lower-troposphere (1000 hPa) are shown on Figure 6.a-b. The ALADIN and ERA-40 reanalysis compare well for larger scales roughly down to 600 km, below which divergence and vorticity from ERA40 dataset start to loose energy, the more the closer to the surface, confirming the kinetic energy spectrum considerations.

As anticipated, on larger scales vorticity field is more energetic than divergence.

However, at wavelengths slightly over 100 km and less, divergence at upper- and middle-levels starts to be almost equally energetic as vorticity. At these scales, motions are even more energetic near the surface than aloft. As such, at 1000 hPa, divergence becomes several times more energetic than vorticity at the same level, suggesting that surface forcing results in creation of unbalanced divergent, rather than balanced rotational meso-β motions. Therefore, the importance of near-surface divergence illustrates a potential constraint of mass-consistent non-divergent models in simulating the near-surface wind climate, if applied over the complex terrain.

3.4 Spectral analysis in temporal domain

Since several measurement stations are located in the proximity of complex terrain and the seashore and characterized with motions of different temporal scales, the success of the analysed models was verified against the measured data using the spectral verification in temporal domain. Spectral verification was achieved through the comparison of spectral power density functions of zonal and meridional wind components, u and v, since typical diurnal rotation of winds (Telišman Prtenjak and Grisogono, 2007) hides the diurnal spectral peak, if spectral analysis is performed with the use of wind speed values. Prior to spectral decomposition, which was made with the use of Welch (1967) method, data was detrended and missing data was provided with the use of regression analysis.

Power spectral density functions for both horizontal wind components for station SLB are shown on Fig. 7a-b. It is first to be noted that DADA spectrum, shown here for reference, is generally similar to ALHR, since mere dynamical adaptation should not have potential to introduce additional energy scales of motion in temporal domain. The largest portion of the measured spectrum is associated with synoptic and mesoscale motions. These large scale motions (here defined as motions of periods > 26 hours) are more energetic for zonal wind component, likely associated primarily with predominantly westerly zonal flow and more complex terrain in meridional directions. While these synoptic circulations are well described with the ALADIN model data, energy of synoptic and mesoscale motions in ERA40 data over station SLB is quite overestimated, especially for the meridional wind component. The overestimation of synoptic energy associated with meridional wind directions is likely due to the non-local influence of the Dinaric Alps (not fully resolved in ERA40 data) further south/southwest of the station. Namely, since Dinaric Alps partially block the southwesterly sirocco winds, channelling those to southeasterly direction over the Adriatic, an unresolved mountain range could contribute to overestimation of these winds over the inland area (Pasarić et al., 2007). The secondary diurnal maximum, underestimated in both ALHR and DADA simulations, is however more accurately described by the ERA-40 data. Finally, the prominent underestimation of the power spectral density functions in the temporal range less then 12 hours appears to hold for all stations and will be discussed later in the text.

The results of spectral decomposition for the coastal stations are shown on Figs 8a-b, 9a-b and 10a-b. Spectral power at coastal stations is overall much higher than for the SLB station over the whole frequency range. For NOV, the ALADIN model data shows the greatest accuracy among all the coastal stations, regardless of the slight underestimation of power spectrum of diurnal motions. The considerable improvement, compared to the global reanalysis, is apparent in all frequency ranges. For station STM, both ERA40 and ALADIN model data appear to underestimate the power of larger scale motions likewise, though there are differences regarding the zonal and meridional wind direction. However, on diurnal scales ALADIN model considerably outperforms the ERA40 data, which appears to be the main added value of downscaling at this station. Finally, on station DUB, ERA40 seems more accurate than the ALADIN model data in synoptic frequency range (see Sec. 3.3 for discussion), the latter having a tendency to underestimate the power of larger-scale motions. However, the shape of ERA40 power spectrum compares unfavourable to well shaped ALADIN power spectrum, showing an increased power on synoptic, at the expense of mesoscale range. Finally, in diurnal range, performance of both models on this station seems reasonable, despite some apparent deficiencies presumably associated with modelled wind direction.

Unlike the SLB station, all coastal stations show the existence of a terciary maximum, presumably associated with land/sea breeze circulation. These motions of semi-diurnal periods (11-13 hr) are reproduced very accurately in the ALADIN model (12 hrs corresponds to time period of the Nyquist frequency for ERA40 data, so comparison is not fully applicable). Last of all, a common feature of the ALADIN model simulations appears to be the underestimation of spectral power of motions with periods less then 12 hours. Similar result was achieved for dynamical downscaling with the ALADIN model over the complex terrain of Slovenia, regardless of the domain size and nesting strategy (Žagar et al., 2006). This suggests ALADIN model is of limited ability to form mesoscale energy on less than semidiurnal temporal scales. Concerning the generous spin-up time (12 hours), it is more likely that low spatial and temporal predictability of motions on these scales and possibly too strong numerical diffusion in the ALADIN model are main contributors to this underestimation. Therefore, though not very relevant for Croatian region, the lack of energy in motions with temporal scales less then 12 hours might constrain the use of current version of the ALADIN mesoscale model in areas where a considerable part of the spectral power exists on the less-then-semidiurnal part of the spectrum.

4. Conclusions

Dynamical downscaling for the wider Croatian region, in part prone to extreme gusty downslope windstorm bora, was performed with the use of ALADIN model driven by the ERA40 reanalysis during a 10-yearly period, in order to get the climatological base for wind energy resource assessment. The modelling system was initiated daily in two subsequent steps: 1) the full ALADIN model integration (ALHR) to 8 km horizontal grid resolution with a 60-min output frequency 2) the simplified model run, so-called dynamical adaptation (DADA), initiated by the ALHR model, to 2 km horizontal grid resolution. All model data was evaluated against the measured data, with both statistical and spectral verification preformed.

Results suggest that wind resource is considerably stronger in the coastal than in continental part of Croatia. Near-surface mean wind speed is the highest in areas of the Vratnik pass and downstream, on the lee sides of the Velebit mountain and on prominent mountain tops. While mountaintops are frequent regions on enhanced wind resource, the former areas, known for bora severity and frequency, clearly identify the primary role of bora in determining the wind climate in the wider area of the eastern Adriatic.

Statistical verification, performed with the use of multiplicative bias (MBIAS) and root-mean square error (RMSE), suggests that the downscaling was quite successful. The accuracy of the ALHR model values is systematically increased compared to ERA40, both in flat and complex coastal terrain, with an exception of DUB station (presumably due to errors related to bilinear interpolation near the land-sea mask). The added value of the so-called dynamical adaptation, compared to ALHR model version, is however notable on all stations analysed. The final downscaling results produced with dynamical adaptation to 2 km horizontal grid resolution show higher accuracy for continental Croatia and station SLB, where systematic error equals 1%, than coastal Croatia and stations NOV, STM and DUB, where mean wind speed value is underestimated for close to 10 %. On the other hand, normalized RMSE values are similar among the analysed stations and equal close to 12 % of mean wind speed.

The scale dependent evaluation, performed with the use of spectral analysis in both spatial and temporal domains, enabled the model assessment on a variety of scales. Kinetic energy spectrum compares well with theoretical and observational evidence gathered in mid-latitudes, with its shape showing no dependence on season. At the upper troposphere (300 hPa) and for scales over several hundreds kilometres, the kinetic energy spectrum acquires k^{-3} dependency for both ERA40 and ALADIN model results. At 700 hPa, the spectrum relaxes to k^{-2}, followed by $k^{-5/3}$ near the surface, illustrating the effect of enhanced trodimensionality of motions and the boundary layer turbulence. In the common part of the wavelength domain, differences between ERA40 and ALADIN data are inexistent for larger wavelengths, but on scales below ~700 km grow as approaching to the ground, where near-surface ERA40 data does not contain enough kinetic energy. On the other hand, a major flaw of the ALADIN model kinetic energy spectrum seems to be an unfavourable steepening of k^{-3} dependency at upper-levels and scales below few hundred kilometres.

As expected, vorticity is more energetic than divergence at the upper-levels, especially at larger scales. However, near the surface and for scales slightly above 100 km and less, divergence spectrum is several times more intensive than vorticity spectrum. This shows that mesoscale simulations contain a considerable amount of energy on meso-β (20-200 km) scales related to near-surface unbalanced divergent motions, illustrating the inherent constraint of mass consistent non-divergent models for assessing the near-surface wind climatology or resource estimate.

Spectral decomposition of measured and modelled data in temporal domain shows reasonable accuracy over the different temporal scales of motion for all model datasets, with a little difference between ALHR and DADA spectra. In continental Croatia, downscaling improves global model spectrum primarily in the synoptic and mesoscale motions, probably due to the non-local influence of the orography of Dinaric Alps to the south. The accuracy of modelled power spectrum varies throughout the coastal stations, showing somewhat underestimated values in the synoptic and mesoscale range. The main benefit of mesoscale modelling is present in well-simulated diurnal and semidiurnal ranges, where the results of dynamical downscaling considerably outperform ERA40 data. Finally, the spectral power of motions with less than semidiurnal periods (not available from ERA40 reanalysis) is strongly underestimated in the mesoscale simulations. Although the portion of power in this frequency range is almost negligible for the analysed stations in Croatia, this model feature might constrain its usage in areas with considerable amount of energy present on these very scales.

Due to the importance of strong mesoscale local winds, such as bora and jugo, for wind climate and resource estimates in the coastal, complex terrain of Croatia, the reduction of remaining uncertainties in numerical modelling of these phenomena confirms essential for the improvement of future higher-resolution dynamical downscaling in the region. While simplified dynamical adaptation proves like a quite an useful and cost-effective alternative at scales of a few kilometers, more detailed dynamical downscaling of wind resource/climate would probably require the use of non-simplified meteorological models on the edge of the large eddy simulation (LES) grid resolutions. Finally, concerning the world-wide appearance of the bora-type flow, the analysis and numerical simulations of bora gustiness and turbulence do remain one of the major research challenges related to both meteorological and wind energy applications in complex terrain.

Acknowledgements: This study was supported by HEP-OIE d.o.o, UKF grant no. 16/08 through the WINDEX project (www.windex.hr) and the project 004-1193086-3036 funded by Ministry of Science, Technology and Sports of Croatia. Authors are grateful to Melita Perčec-Tadić for her assistance related to graphical presentation of the mean wind speed map.

References

Bajić, A., 1989: Severe bora on the northern Adriatic. Part I: Statistical analysis. *Rasprave-Papers*, **24**, 1-9.

Beck A., B. Ahrens and K. Stadlbacker, 2004: Impact of nesting strategies in dynamical downscaling of reanalysis data. *Geophys. Res. Let.*, **31**, L19101, doi:10.1029/2004GL020115.

Belušić, D. and Z. B. Klaić, 2006: Mesoscale dynamics, structure and predictability of a severe Adriatic bora case**.** *Meteorol. Z.*, **15**, 157-168.

Boer, G. J. and T. G.. Shepherd, 1983: Large-scale two-dimensional turbulence in the atmosphere. *J. Atmos. Sci.,* **40,** 164–184.

Bubnova R., G. Hello, P. Benard and J. F. Geleyn, 1995: Integration of fully elastic equations cast in the hydrostatic pressure terrain-following coordinate in the framework of ARPEGE/ALADIN NWP system. *Mon. Wea. Rev.*, **123**, 515-535.

Cavaleri, I., L. Bertotti and N. Tescaro, 1997: The modelled wind climatology of the Adriatic sea, *Theor. App. Climatol.*, **56**, 231-254.

Charney, J. G.., 1971: Geostrophic turbulence. *J. Atmos. Sci.,* **28,** 1087–1095.

Davies, H. C., 1976: A lateral boundary formulation for multi-level prediction models. *Quart. J. Roy. Meteorol. Soc.*, **102**, 405-418.

Gage K. S. and G. D. Nastrom, 1986: Theoretical Interpretation of Atmospheric Wavenumber Spectra of Wind and Temperature Observed by Commercial Aircraft During GASP. *J. Atmos. Sci.*, **43**, 729-740.

Geleyn, J. F., 1987: Use of a modified Richardson number for parametrizing the effect of shallow convection. In: Matsuno Z. (ed.), Short and medium range weather prediction, Special volume of *J. Meteor. Soc. Japan*, 141-149.

Geleyn, J. F., C. Girard and J.-F. Louis, 1982: A simple parametrization of moist convection for large-scale atmospheric models. *Beitr. Phys. Atmos.*, **55**, 325-334.

Geleyn, J. F. and A. Hollingsworth, 1979: An economical analytical method for computation of the interaction between scattering and line apsorption of radiation. *Contr. Atmos. Phys.*, **52**, 1-16.

Giard, D. and E. Bazile, 2000: Implementation of a new assimilation scheme for soil and surface variables in a global NWP model. *Mon. Wea. Rev.*, **128**, 997-1015.

Göhm, A., G. J. Mayr, A. Fix and A. Giez, 2008: On the onset of Bora and the formation of rotors and jumps near a mountain gap. *Q. J .R. Meteorol. Soc.,* **134**, 21-46.

Grisogono B. and D. Belušić, 2009: A review of recent advances in understanding the meso- and microscale properties of the severe Bora wind. *Tellus*, **61A**, 1-16.

Horvath, K., Y.-L. Lin and B. Ivančan-Picek, 2008: Classification of Cyclone Tracks over Apennines and the Adriatic Sea. *Mon. Wea. Rev.*, **136**, 2210-2227.

Horvath, K., S. Ivatek-Šahdan, B. Ivančan-Picek and V. Grubišić, 2009: Evolution and structure of two severe cyclonic Bora events: Contrast between the northern and southern Adriatic. *Wea. Forecasting*, **24**, 946-964.

Ivatek-Šahdan, S. and M. Tudor, 2004: Use of high-resolution dynamical adaptation in operational suite and research impact studies. *Meteorol. Z.,* **13**, 99-108.

Jurčec, V., B., Ivančan-Picek, V. Tutiš and V. Vukičević, 1996: Severe Adriatic Jugo wind. *Meteorol. Z.*, **5**, 67-75.

Kållberg P., A. Simmons, S. Uppala and M. Fuentes, 2004: The ERA-40 archive. *ECMWF ERA-40 Project Report Series*, **17**, 1-35.

Kessler, E., 1969: On distribution and continuity of water substance in atmospheric circulations. *Met. Mon. Am. Met. Soc.*, **10**, 84 pp.

Klemp J. B. and D. R. Durran, 1987: Numerical modelling of Bora winds. *Meteorol. Atmos. Phys.*, **36**, 215-227.

Kraichnan, R. H., 1967: Inertial ranges in two-dimensional turbulence. *Phys. Fluids,* **10,** 1417–1423.

Lilly, D. K., 1969: Numerical simulation of two-dimensional turbulence. *Phys. Fluids,* **12** (Suppl. II), 240–249.

Lindborg, E., 1999: Can the atmospheric kinetic energy spectrum be explained by two-dimensional turbulence? *J. Fluid Mech.,* **388,** 259–288.

Louis J.-F., M. Tiedke and J. F. Geleyn, 1982: A short history of PBL parametrisation at ECMWF. *Proceedings from the ECMWF Workshop on Planetary Boundary Layer Parametrisation*, 59 – 79.

Lynch, P. and X. Y. Huang, 1994: Diabatic initialization using recursive filters. *Tellus*, **46A**, 583-597.

Machenhauer, B. and J. E. Haugen, 1987: Test of spectral limited area shallow water model with time-dependent lateral boundary conditions and combined normal mode/semi-Lagrangiean time integration schemes. *ECMWF Workshop Proceedings: Techniques for horizontal discretization in numerical weather prediction models.* Reading, UK, 2-4 November 1987, pp. 361-377.

Makjanić, B, 1976: A short account of the climate of the town Senj. *Local Wind Bora* (M. M. Yoshino ed.). Univ. of Tokyo Press, Tokyo, 145-152.

Mass, C. F., D. Ovens, K. Westrick and B. A. Colle, 2002: Does increasing horizontal resolution produce more skillful forecast? *Bull. Am. Meteorol. Soc.*, **83**, 407–430.

Nastrom, G. D., and K. S. Gage, 1985: A climatology of atmospheric wavenumber spectra of wind and temperature observed by commercial aircraft. *J. Atmos. Sci.,* **42,** 950–960.

Pasarić Z., D. Belušić and Z. B. Klaić, 2007: Orographic influences on the Adriatic sirocco wind. *Ann. Geophys.*, **25**, 1263-1267.

Poje, D., 1992: Wind persistence in Croatia. *Int. J. Climatol.*, **12**, 569-582.

Rife, D. L., Davis, C. A. and Liu, Y. 2004. Predictability of low-level winds by mesoscale meteorological models. *Mon. Wea. Rev.* **132**, 2553–2569.

Ritter, B. and J. F. Geleyn, 1992: A comprehensive radiation scheme for numerical weather prediction models with potential applications in climate simulations. *Mon. Wea. Rev.*, **120**, 303-325.

Simmons, A. J. and D. M. Burridge, 1981: An energy and angular momentum conserving vertical finite-difference scheme and hybrid vertical coordinate. *Mon. Wea. Rev.*, **109**, 758-766.

Skamarock, W. C., 2004: Evaluating Mesoscale NWP Models Using Kinetic Energy Spectra. *Mon. Wea. Rev.*, **132**, 3019-3032.

Smith R. B., 1985: On severe downslope winds. *J. Atmos. Sci.*, **42**, 2597-2603.

Smith, R. B., 1987: Aerial observations of the Yugoslavian bora. *J. Atmos. Sci.*, **44**, 269-297.

Telišman Prtenjak, M. and B. Grisogono, 2007: Sea/land breeze climatological characteristics along the northern Croatian Adriatic coast. *Theor. App. Climatol.*, **90**, 201-215.

Welch P. D., 1967: The use of fast Fourier transform for the estimation of power spectra: a method based on time averaging over short, modified periodograms. *IEEE Transactions on Audio Electroacoustics*, Vol. **AU-15** (6), 70-73.

Wilks, D. S., 2006. Statistical Methods in the Atmospheric Sciences, 2nd Ed. *International Geophysics Series*, **59**, Academic Press, 627 pp.

Yoshino M. M., 1976: *Local Wind Bora*. Univ. of Tokyo Press, Tokyo, Japan.

Zaninović, K., M. Gajić-Čapka, M. Perčec-Tadić et al., 2008: *Klimatski atlas Hrvatske / Climate atlas of Croatia 1961-1990, 1971-2000*. Državni hidrometeorološki zavod, Zagreb, 200 str.

Žagar N., M. Žagar, J. Cedilnik, G. Gregorič and J. Rakovec, 2006: Validation of mesoscale low-level winds obtained by dynamical downscaling of ERA-40 over complex terrain. *Tellus*, **58A**, 445-455.

Žagar M. and J. Rakovec, 1999: Small-scale surface wind prediction using dynamic adaptation. *Tellus*, **51A**, 489-504.

Figure captions:

Figure 1: The integration domain of the ALADIN model at 8 km (larger shaded area) and 2 km (inner shaded area) grid resolution with associated digital elevation terrain model as well as geographic features and measurement stations referred to in the text.

Figure 2: Spatial distribution of 10-yearly mean wind speed (1992-2001) [ms^{-1}] at 10 m AGL, as a direct model output of dynamical adaptation at 2 km horizontal grid resolution.

Figure 3.a-d: Monthly variation of mean multiplicative bias (MBIAS) of modeled wind speed at 10 m AGL for stations Slavonski Brod (SLB), Novalja (NOV), Split Marjan (STM) and Dubrovnik (DUB). Note the change in scale for station SLB.

Figure 4.a-d: Monthly variation of root-mean square error (RMSE, ms-1) at 10 m AGL for stations Slavonski Brod (SLB), Novalja (NOV), Split Marjan (STM) and Dubrovnik (DUB). For easier intercomparison, RMSE was calculated with a 6-hourly frequency for all model data.

Figure 5.a-b: Normalized kinetic energy spectrum for ERA40 (EC) and ALHR (AL) data at a) 300 hPa, 700 hPa and 1000 hPa, and b) its seasonal variability at 300 hPa and 1000 hPa.

Figure 6.a-b: Spectral energy density for ERA40 (EC) and ALHR (AL) data at 300 hPa, 700 hPa and 1000 hPa for a) relative vorticity b) divergence.

Figure 7a-b: Power spectrum of measured and modeled (ERA40, ALHR and DADA data) a) zonal and b) meridional wind components for station Slavnoski Brod (SLB).

Figure 8a-b: Power spectrum of measured and modeled (ERA40, ALHR and DADA data) a) zonal and b) meridional wind components for station Novalja (NOV).

Figure 9a-b: Power spectrum of measured and modeled (ERA40, ALHR and DADA data) a) zonal and b) meridional wind components for station Split Marjan (STM).

Figure 10a-b: Power spectrum of measured and modeled (ERA40, ALHR and DADA data) a) zonal and b) meridional wind components for station Dubrovnik (DUB).

Table captions:

Table 1: Measured mean wind speed at 10 m AGL as well as multiplicative systematic error (MBIAS) and root-mean square error (RMSE) as inferred from ERA40, ALHR and DADA datasets with 6-hourly frequency during 2001. for stations Slavonski Brod (SLB), Novalja (NOV), Split Marjan (STM) and Dubrovnik (DUB). A unit MBIAS (MBIAS=1) points to modeled dataset with no systematic error, while MBIAS > (<) 1 indicates the overestimation (underestimation) of modeled data. For reference, 1-hourly values and statistics for ALHR and DADA datasets are given as well.

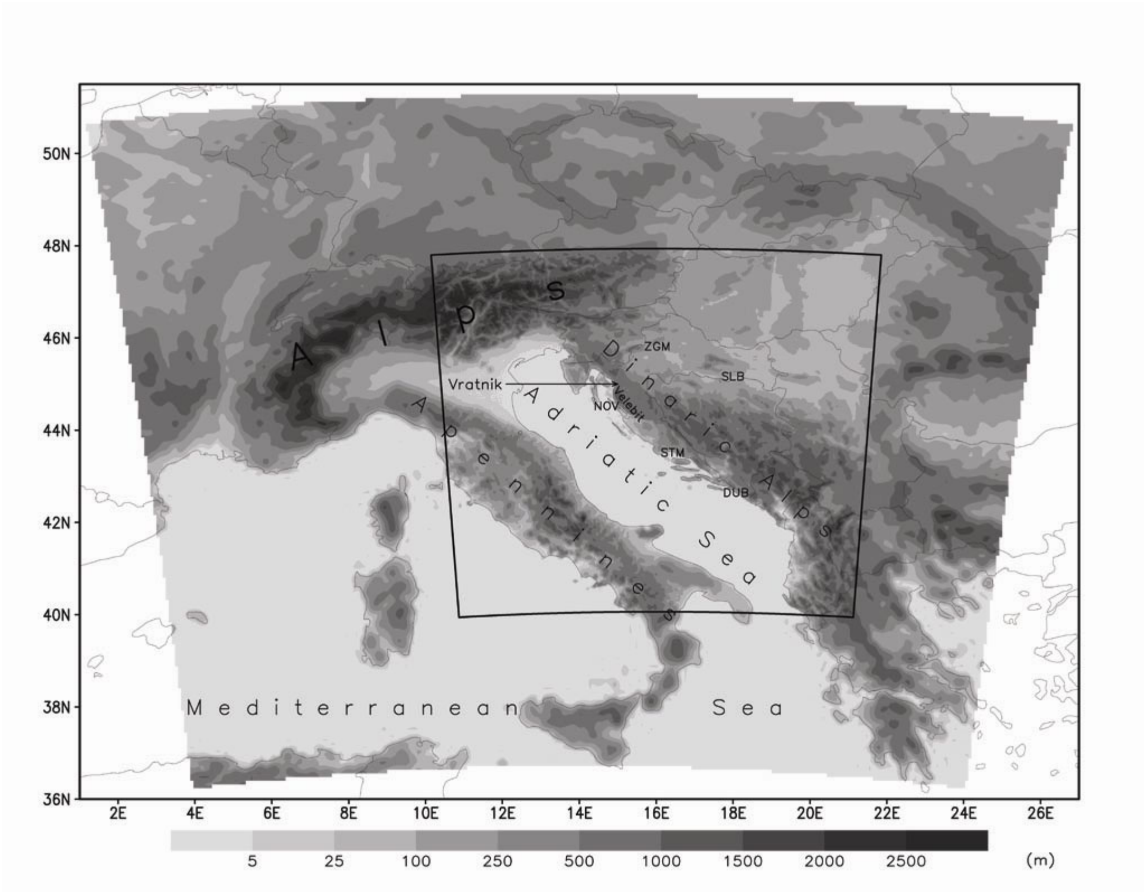

Figure 1: The integration domain of the ALADIN model at 8 km (larger shaded area) and 2 km (inner shaded area) grid resolution with associated digital elevation terrain model as well as geographic features and measurement stations referred to in the text.

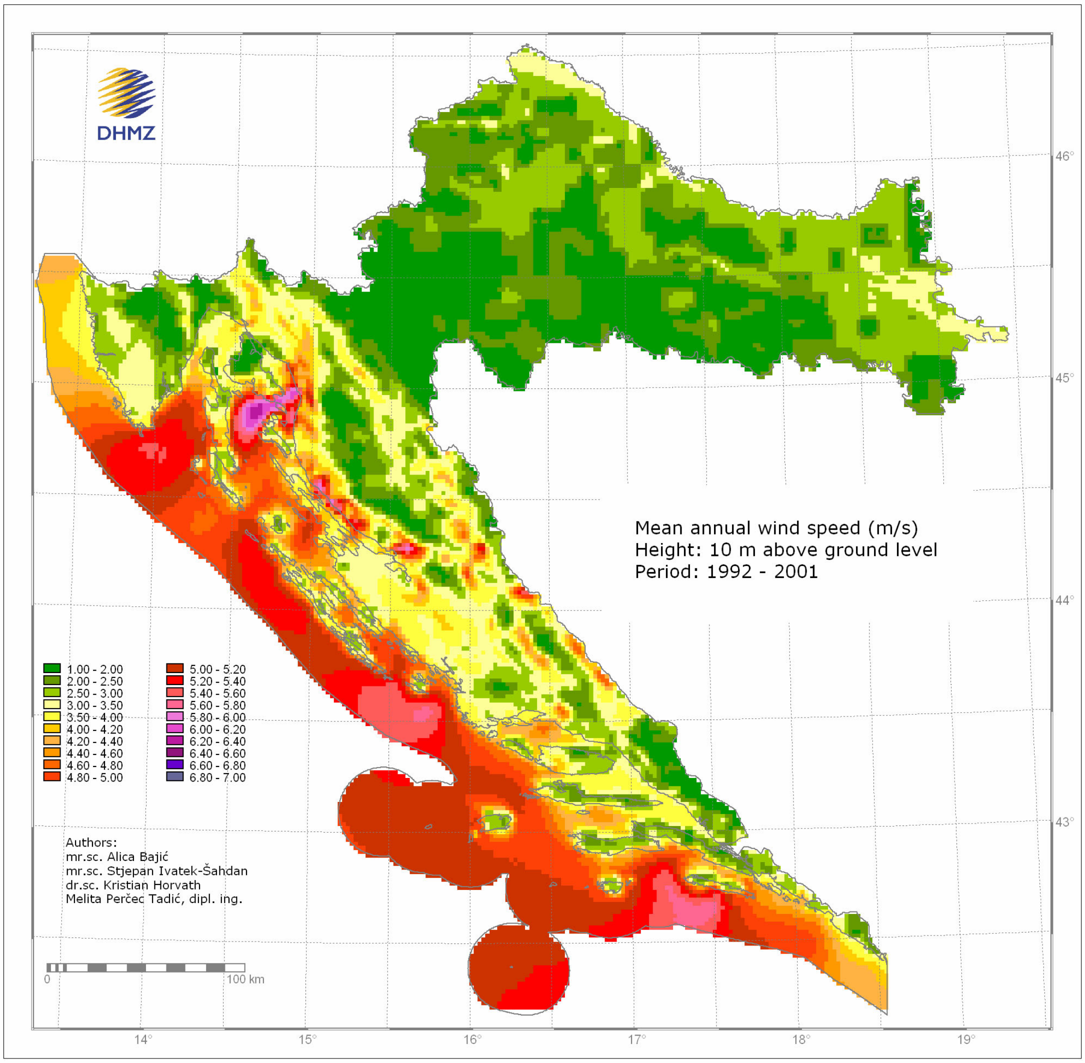

Figure 2: The spatial distribution of 10-yearly (1992-2001) wind speed at 10 m AGL [ms^{-1}], as a direct model output of dynamical adaptation at 2 km horizontal grid resolution.

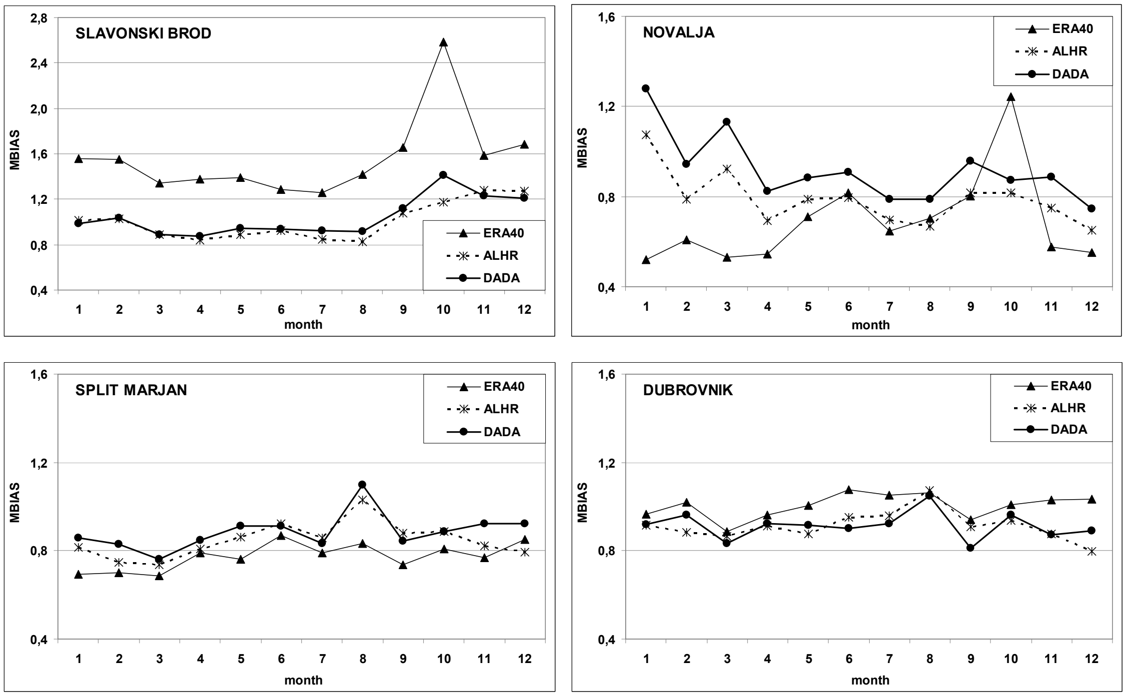

Figure 3.a-d: Monthly variation of mean multiplicative bias (MBIAS) of modeled wind speed at 10 m AGL for stations Slavonski Brod (SLB), Novalja (NOV), Split Marjan (STM) and Dubrovnik (DUB). Note the change in scale for station SLB.

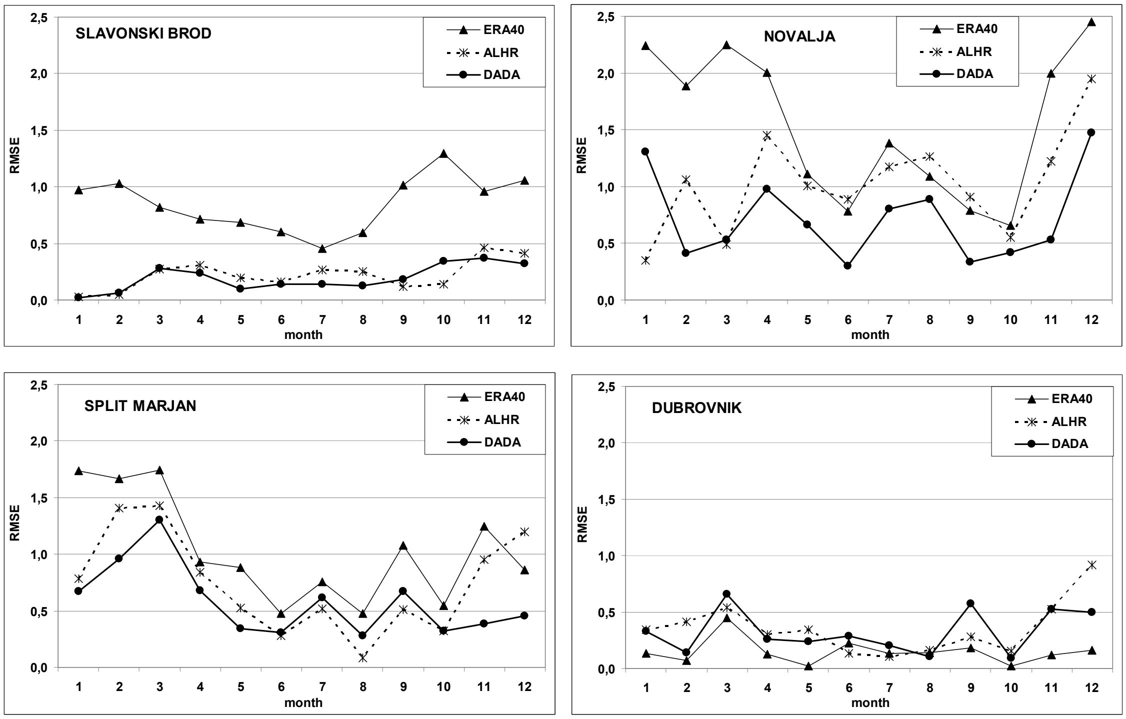

Figure 4.a-d: Monthly variation of root-mean square error (RMSE, ms-1) at 10 m AGL for stations Slavonski Brod (SLB), Novalja (NOV), Split Marjan (STM) and Dubrovnik (DUB). For easier intercomparison, RMSE was calculated with a 6-hourly frequency for all model data.

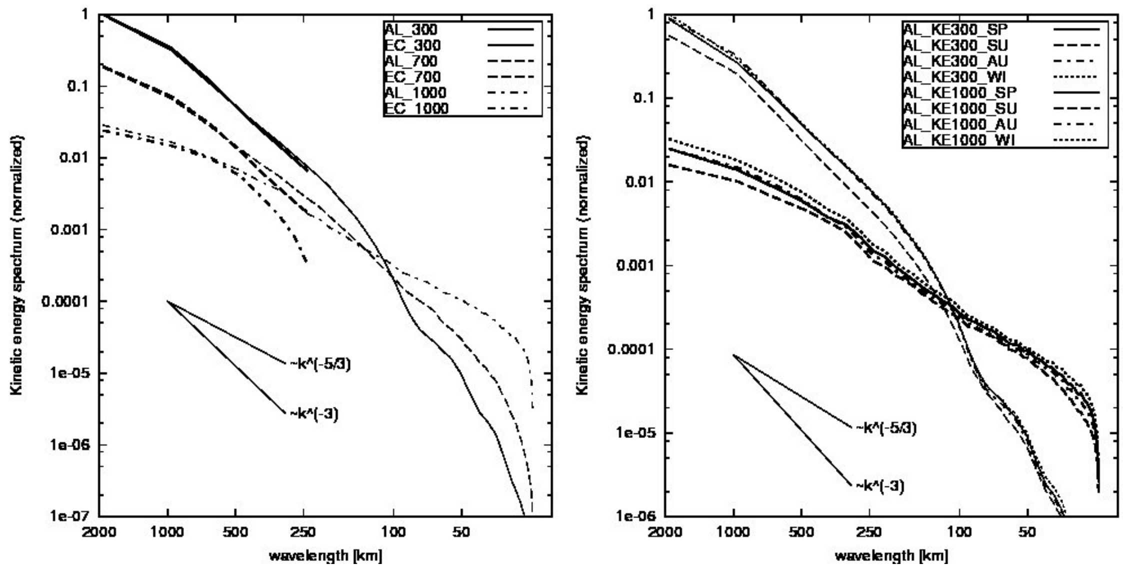

Figure 5.a-b: Normalized kinetic energy spectrum for ERA40 (EC) and ALHR (AL) data at a) 300 hPa, 700 hPa and 1000 hPa, and b) its seasonal variability at 300 hPa and 1000 hPa.

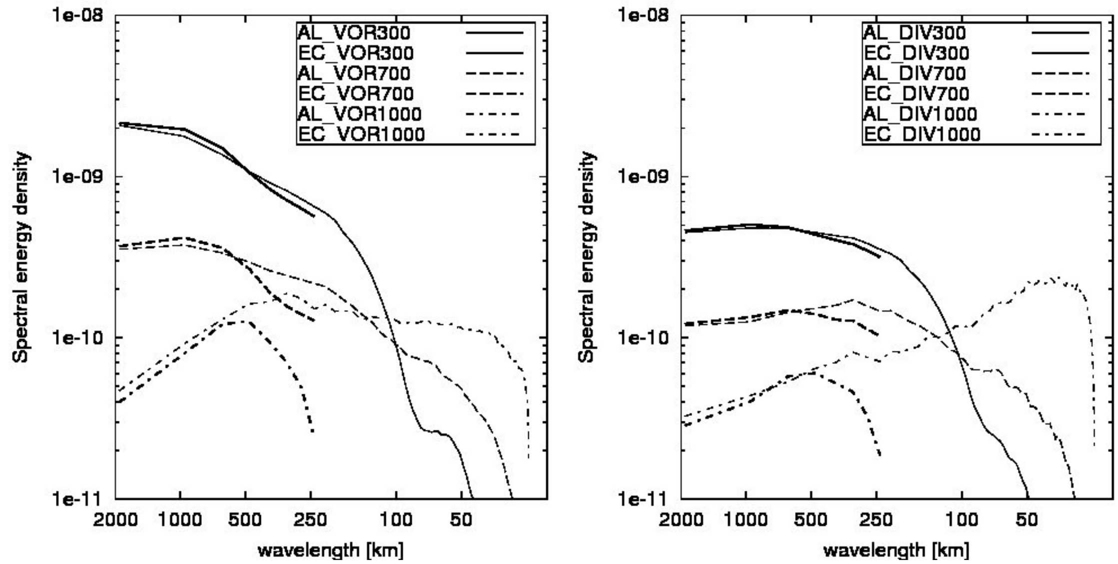

Figure 6.a-b: Spectral energy density for ERA40 (EC) and ALHR (AL) data at 300 hPa, 700 hPa and 1000 hPa for a) relative vorticity b) divergence.

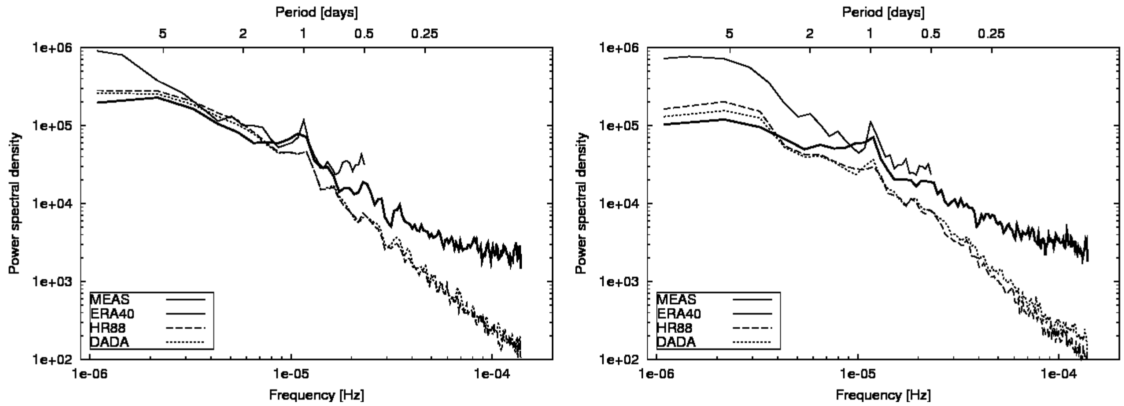

Figure 7a-b: Power spectrum of measured and modeled (ERA40, ALHR and DADA data) a) zonal and b) meridional wind components for station Slavnoski Brod (SLB).

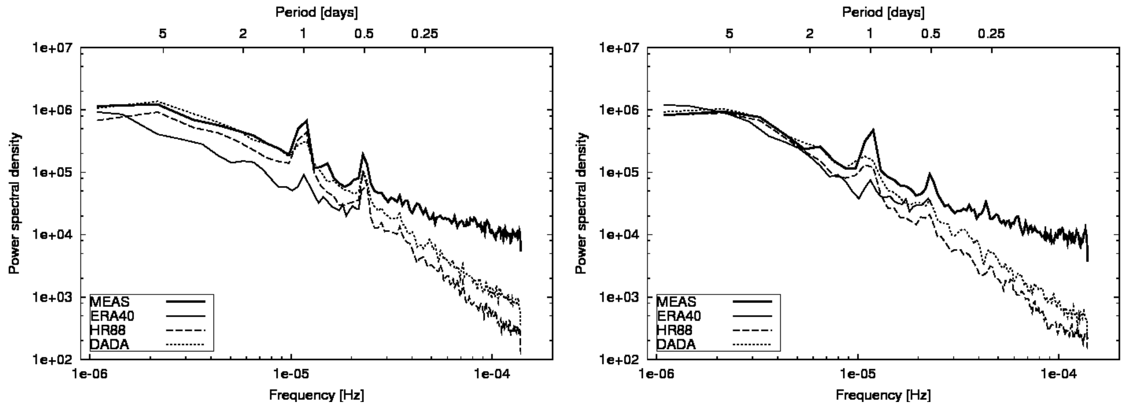

Figure 8a-b: Power spectrum of measured and modeled (ERA40, ALHR and DADA data) a) zonal and b) meridional wind components for station Novalja (NOV).

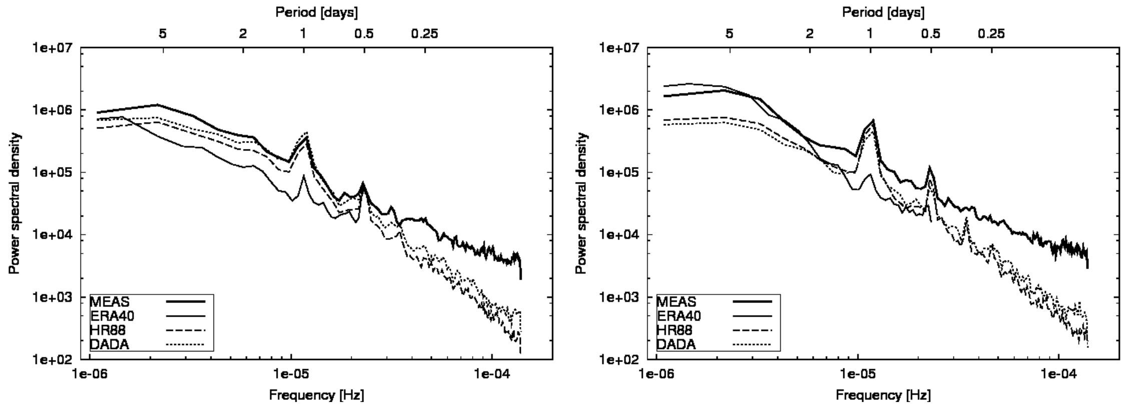

Figure 9a-b: Power spectrum of measured and modeled (ERA40, ALHR and DADA data) a) zonal and b) meridional wind components for station Split Marjan (STM).

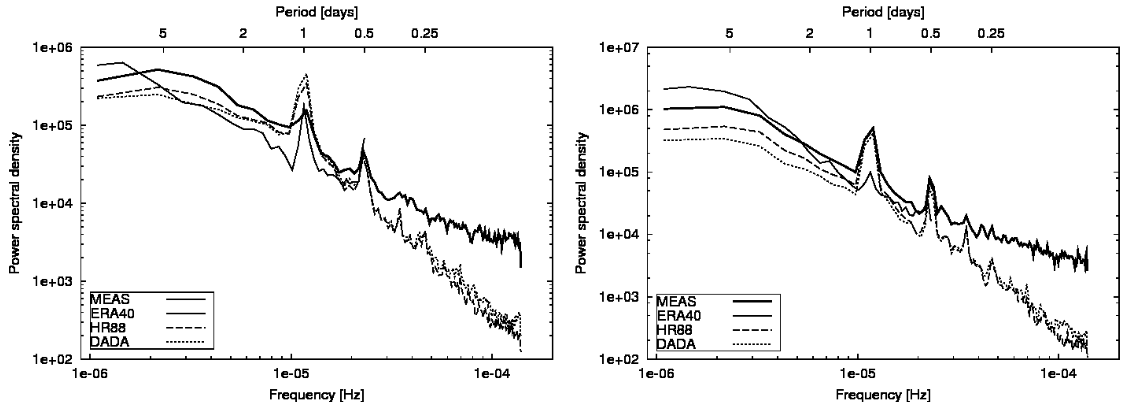

Figure 10a-b: Power spectrum of measured and modeled (ERA40, ALHR and DADA data) a) zonal and b) meridional wind components for station Dubrovnik (DUB).

Table 1: Measured mean wind speed at 10 m AGL as well as multiplicative systematic error (MBIAS) and root-mean square error (RMSE) as inferred from ERA40, ALHR and DADA datasets with 6-hourly frequency during 2001. for stations Slavonski Brod (SLB), Novalja (NOV), Split Marjan (STM) and Dubrovnik (DUB). A unit MBIAS (MBIAS=1) points to modeled dataset with no systematic error, while MBIAS > (<) 1 indicates the overestimation (underestimation) of modeled data. For reference, 1-hourly values and statistics for ALHR and DADA datasets are given as well.

	O-6	**MBIAS-6**			**RMSE-6**			**O-1**	**MBIAS-1**		**RMSE-1**	
	ms^{-1}	ERA6	AL6	DA6	ERA6	AL6	DA6	ms^{-1}	AL1	DA1	AL1	DA1
SLB	1.74	1.51	0.99	1.01	0.85	0.22	0.19	1.72	0.99	0.99	0.21	0.21
NOV	4.26	0.69	0.79	0.92	1.55	1.03	0.73	4.32	0.78	0.91	1.04	0.71
STM	4.42	0.78	0.85	0.89	1.12	0.73	0.58	4.40	0.84	0.87	0.75	0.56
DUB	3.31	1.00	0.91	0.91	0.18	0.35	0.33	3.35	0.88	0.90	0.41	0.35